

Light curve solutions of six short-period binaries and peculiarities of two of them, NSVS 3640326 and V1007 Cas

D. Kjurkchieva¹, V. Popov², N. Petrov³ and E. Ivanov²

¹ *Department of Physics, Shumen University, 115, Universitetska Str., 1712 Shumen, Bulgaria, (E-mail: d.kjurkchieva@shu-bg.net)*

² *IRIDA Observatory, 17A Prof. Asen Zlatarov str., Sofia, Bulgaria*

³ *Institute of Astronomy and National Astronomical Observatory, Bulgarian Academy of Sciences, 72, Tsarigradsko Shose Blvd., 1784 Sofia, Bulgaria*

Received: November 24, 2014; Accepted: February 17, 2015

Abstract. Photometric observations in Sloan g' and i' bands of six binaries with orbital periods of 6–8 hours are presented. One of them is a newly discovered eclipsing system. NSVS 3640326, V1007 Cas and V568 Peg have fillout factors above 0.26 and their components differ in mass more than 2 times. All systems revealed the O'Connell effect that was reproduced by cool spots on the side surfaces of their primary components. The light curves of NSVS 3640326 and V1007 Cas seem unusual due to their flat MinI. This peculiarity implies an extremely weak limb-darkening effect of their primaries. Another peculiarity of V1007 Cas is that its secondary is cooler, but bigger and considerably more massive, than its primary. Moreover, V1007 Cas turned out to be well below the line representing the mass-luminosity relation for the MS stars on the mass ratio – luminosity ratio diagram.

Key words: stars: binaries: eclipsing – stars: individual (NSVS 3640326, V1007 Cas, NSVS 1776195, UCAC4-525-135123, NSVS 113026, V568 Peg)

1. Introduction

Most W UMa stars consisting of solar-type components have orbital periods within $0.25 \text{ d} < P < 0.7 \text{ d}$. They are recognized by continuous brightness variations and nearly equal minima depths. The short orbital periods of these binaries mean small orbits and synchronized rotation and orbital revolution.

Both components of the W UMa stars overflow their Roche lobes and form a common envelope of material, which causes the stars to have the same surface temperature to within 100-200 K (Lucy 1968). It is assumed that two stars with a common envelope cannot be in stable equilibrium, but these systems oscillate between states of the full and marginal contact (Flannery 1976; Lucy 1976; Robertson, Eggleton 1977).

The formation of contact binary systems is not well understood. Pribulla, Rucinski (2006) state that it is not possible for a system with a period below

one day to be created in a binary form. A third (distant) companion is necessary for formation of such objects.

The further evolution of short-period detached systems probably is characterized by angular momentum loss (AML) through a magnetized wind with a single mass-ratio reversal (Stepien 2006), while that of contact binaries by combination of AML and mass-ratio oscillations (Qian 2003).

The investigation of the contact binary systems is important for the modern astrophysics for at least three reasons.

(1) The W UMa stars are natural laboratories for the study of late stages of the stellar evolution connected with the processes of mass and angular momentum loss, merging or fusion of the stars (Martin *et al.*, 2011).

(2) The contact binary stars have an unique and useful property: the period-color relation. The similar temperatures of the components through a combination of the Kepler third law and the radius-color relationship for Main Sequence (MS) stars lead to a period-color-luminosity relation (Rucinski 1994; Rucinski 1996; Rucinski, Duerbeck 1997; Klagyivik, Csizmadia 2004; Gettel *et al.* 2006; Eker *et al.*, 2008). This makes contact binaries useful tracers of distance and galactic structure, especially on small scales.

(3) The contact binaries present a numerous family, although their space density and distribution are still debated. Rucinski (2002) found a density of $1.0 * 10^{-5} \text{pc}^{-3}$, or 1/500 MS stars, in the solar neighborhood. However, the previous estimate of 1/130 MS stars based on OGLE-I data for more distant stars in the Galactic disk is quite different (Rucinski 1998). This discrepancy may be an indication of an uneven distribution of the contact binary fraction across the Galaxy.

The General Catalog of Variable Stars (GCVS) labels 845 stars as EW type variables (Samus *et al.*, 2004). The catalog of Pribulla *et al.* (2003) contains 361 galactic EW and EB type variables. Gettel *et al.* (2006) created a new catalog of 1022 contact binary stars from the ROTSE-I database and estimated their space density as $1.7 * 10^{-5} \text{pc}^{-3}$.

Although the continuously varying light curves make the contact binaries detectable within a large range of inclinations, the statistics of W UMa stars with short periods is quite poor (Terrell *et al.*, 2012). There are two reasons for this insufficiency: (a) the period distribution of binaries reveals a very sharp decline in the number of systems with periods below 0.27 days (Drake *et al.*, 2014); (b) the short-period binaries are late stars and thus faint objects for a detailed study.

In this paper we present photometric observations and light curve solutions of six binaries with orbital periods within 6–8 hours: NSVS 3640326, V1007 Cas (\equiv NSVS 3687570 \equiv CSV 8 \equiv NSV 49 \equiv GSC 03258-00448), NSVS 1776195, UCAC4-525-135123, NSVS 113026 (\equiv 2MASS J21273926+7639576 \equiv GSC 04599-00229 \equiv NSVS 1279949 \equiv NSVS 1318204 \equiv NSVS 1406039 \equiv UCAC4 834-018531 \equiv USNO-B1.0 1666-0103264), V568 Peg. Five of our targets are known binaries from the NSVS database (Wozniak *et al.*, 2004), while one of

Table 1. Old parameters of our targets.

Target Name	RA 2000	Dec 2000	Period [d]	V [mag]	Ampl [mag]	Ref
1 NSVS 3640326	00 04 14.22	+43 18 03.4	0.31129014	12.57	0.60	1
2 V1007 Cas	00 08 03.43	+51 08 02.8	0.3320075	12.00	0.44	2, 3, 4
3 NSVS 1776195	01 59 34.73	+53 02 48.2	0.17604293	11.38	0.17	1
4 UCAC4-525-135123	20 36 52.63	+14 56 43.3	0.25158	15.50	0.66	new
5 NSVS 113026	21 27 39.27	+76 39 57.6	0.281973	12.70	0.25	5
6 V568 Peg	23 08 13.42	+33 03 02.1	0.247074	12.90	0.45	6

References: 1 – Shaw *et al.* (Finding periodic variables in the NSVS); 2 – Otero *et al.*, 2005; 3 – Gettel *et al.*, 2006; 4 – Diethelm, 2013; 5 – Wozniak *et al.*, 2004; 6 – Khruslov, 2008.

them is a newly discovered binary. Table 1 gives the coordinates of our targets and available information for their light variability.

2. Observations

Our CCD photometric observations of the targets in Sloan g' , i' bands were carried out at Rozhen Observatory with the 30-cm Ritchey Chretien Astrograph (located in the *IRIDA South* dome) using a CCD camera ATIK 4000M (2048 × 2048 pixels, 7.4 μm /pixel, field of view 40 x 40 arcmin). Information on our observations is given in Table 2.

The photometric data were reduced by *AIP4WIN2.0* (Berry, Burnell 2006). We performed aperture ensemble photometry with the software *VPHOT* using more than six standard stars in the observed field of each target. Table 7 in the *Appendix* gives their coordinates and magnitudes from the catalogue UCAC4 (Zacharias *et al.*, 2010).

3. Light curve solutions

We solved the Rozhen light curves of the six targets using the code *PHOEBE* (Prsa, Zwitter, 2005) by the following procedure.

We used the traditional convention the MinI (phase 0.0) to be the deeper light minimum and the star that is eclipsed at MinI to be the primary component.

We determined in advance the mean temperatures T_m of the binaries (Table 3) by their infrared color indices ($J-K$) from the 2MASS catalog and the calibration color-temperature given by Tokunaga (2000).

At the first step we adopted $T_1 = T_m$ and searched for solutions for fixed T_1 varying the initial epoch T_0 , period P , secondary temperature T_2 , orbital inclination i , mass ratio q and potentials $\Omega_{1,2}$.

We adopted coefficients of gravity brightening $g_1 = g_2 = 0.32$ and the reflection effect $A_1 = A_2 = 0.5$ appropriate for late-type stars, while the limb-

Table 2. Journal of the Rozhen photometric observations.

Target	Date	Exposure (g', i') [sec]	Number (g', i')	Error (g', i') [mag]
1	2014 Oct 12	60, 90	51, 45	0.004, 0.006
	2014 Oct 13	60, 90	155, 167	0.004, 0.005
	2014 Oct 19	60, 90	158, 175	0.004, 0.005
2	2014 Oct 20	60, 90	183, 137	0.003, 0.004
	2014 Nov 02	60, 90	194, 194	0.004, 0.005
3	2014 Oct 01	30, 60	165, 182	0.003, 0.004
	2014 Oct 10	30, 60	144, 144	0.003, 0.003
	2014 Oct 11	30, 60	159, 151	0.003, 0.003
4	2014 Aug 15	90, 90	92, 92	0.021, 0.027
	2014 Aug 18	90, 90	87, 85	0.018, 0.025
5	2014 Aug 07	90, 90	51, 50	0.008, 0.009
	2014 Aug 08	90, 90	72, 69	0.007, 0.008
	2014 Aug 09	90, 90	90, 88	0.006, 0.007
	2014 Aug 12	90, 90	109, 109	0.004, 0.006
	2014 Aug 14	90, 90	93, 92	0.004, 0.006
	2014 Aug 15	90, 90	109, 108	0.004, 0.006
6	2014 Sept 24	90, 90	136, 136	0.005, 0.007
	2014 Sept 29	90, 90	51, 49	0.005, 0.007
	2014 Sept 30	90, 90	150, 149	0.005, 0.007
	2014 Oct 11	90, 90	150, 149	0.007, 0.007

Table 3. Parameters of variability of the targets according to the Rozhen data. Their J - K colors from the 2MASS catalog are used for determination of the mean temperatures T_m .

Target	T_0 -2450000	Period [d]	$\Delta g'$ [mag]	$\Delta i'$ [mag]	J - K [mag]	T_m [K]
1	6972.546000(77)	0.419420000(3)	0.638	0.591	0.500	5370
2	6972.342000(17)	0.251206000(2)	0.606	0.564	0.700	4450
3	7005.383500(19)	0.348888080(3)	0.122	0.131	0.226	6700
4	7016.338000(24)	0.280628000(3)	0.701	0.589	0.531	5240
5	7016.428000(11)	0.322424000(2)	0.266	0.237	0.400	5700
6	7011.316500(21)	0.334562000(1)	0.681	0.568	0.419	5650

darkening coefficients for each component and each color were updated according to the tables of Van Hamme (1993).

In order to reproduce the O'Connell effect, we added cool spots on the stellar surfaces of the primary components and varied their parameters (longitude λ , latitude β , angular size α and temperature factor κ).

To adjust the stellar temperatures T_1 and T_2 around the mean value T_m , we used the formulae

$$T_1^c = T_m + \frac{c\Delta T}{c+1}, \quad (1)$$

$$T_2^c = T_1 - \Delta T, \quad (2)$$

where $c = l_2/l_1$ (luminosity ratio) and ΔT (difference of temperatures of the components) were determined from the last *PHOEBE* solution. We derived expressions (1-2) on the basis of formula (4) of Coughlin *et al.* (2011).

To obtain the best solution, we varied finally the stellar temperatures slightly around the calculated values $T_{1,2}^c$ as well as the parameters i , q and $\Omega_{1,2}$.

Table 4 contains the derived parameters by this procedure, where $r_{1,2}$ are relative (volume) stellar radii and $l_{1,2}$ are relative luminosities of the stellar components. The values of T_0 and P are given in Table 3, while those of the spot parameters are shown in Table 5.

The errors of the obtained parameters are the formal *PHOEBE* errors.

The synthetic light curves corresponding to our solutions are shown in Figs. 1–6 as continuous lines.

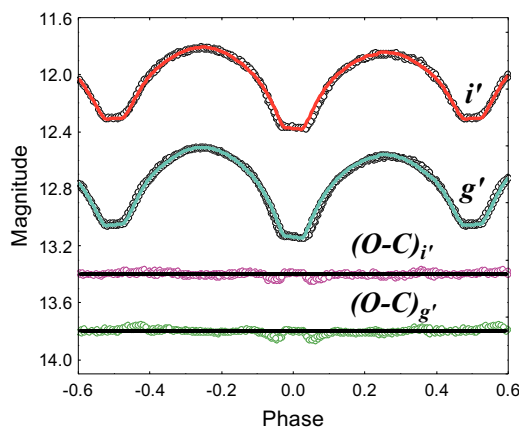


Figure 1. The folded light curves of NSVS 3640326 with their fits and the corresponding residuals (shifted vertically by an arbitrary number to save space). A color version of this figure is available in the online journal.

4. Analysis of the results

The analysis of the light curve solutions of the Rozhen data led to several conclusions.

(1) Our photometric data revealed that the period of NSVS 1776195 is 2 times longer than the published one (Table 1).

(2) The amplitudes of variability of V1007 Cas and V0568 Peg turned out to be considerably bigger than the published ones. We assume that the reason for this discrepancy is the low angular resolution of the published photometric

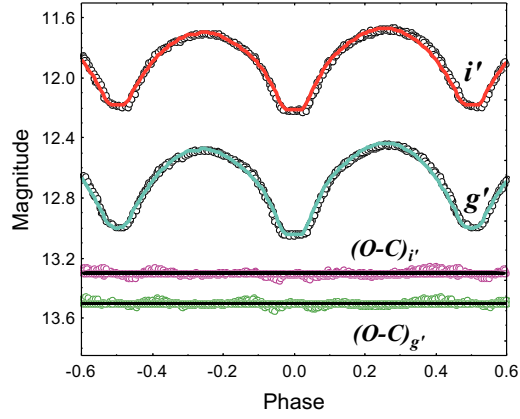


Figure 2. Same as Fig. 1 for V1007 Cas.

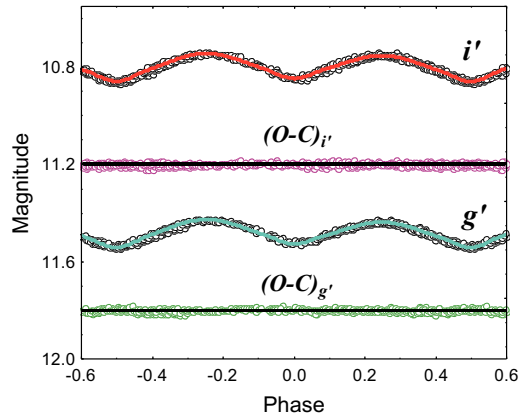


Figure 3. Same as Fig. 1 for NSVS 1776195.

observations by the small NSVS telescopes ($14.4''\text{pixel}^{-1}$) that prevents separation of two neighboring stars. A close nonvariable star may enter the same pixel or aperture during the photometric measurements of the variable and thus reduce its amplitude of variability.

(3) The light variabilities of NSVS 1776195 and NSVS 113026 are almost ellipsoidal (the eclipses are quite grazing).

(4) Five targets are overcontact binaries, one target (NSVS 1776195) is an almost contact system (Table 4).

(5) The stellar components of all targets are of G and K spectral types.

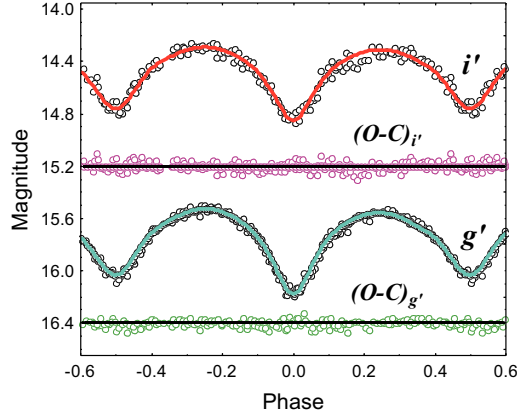


Figure 4. Same as Fig. 1 for UCAC4-525 135123.

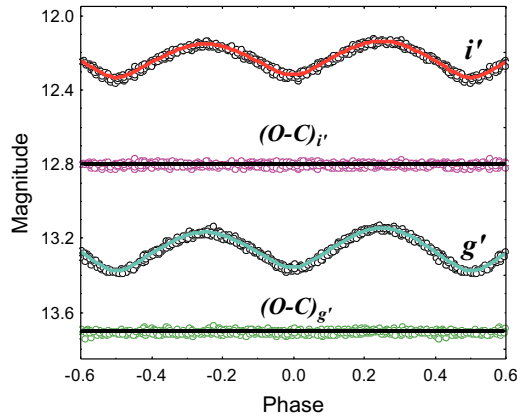


Figure 5. Same as Fig. 1 for NSVS 113026.

(6) The masses of the components of NSVS 3640326, V1007 Cas and V568 Peg differ more than 2 times from each other. Only these targets are with the biggest fillout factors.

(7) The temperature difference of the components of the targets are up to 400 K, i.e. they are almost in thermal contact.

(8) All binaries revealed the O'Connell effect that was reproduced by big cool spots (Table 5) on the side surfaces of their primary components. These spots are manifestation of the magnetic activity of the targets.

(9) The best fit in the two colors required a contribution of third light l_3

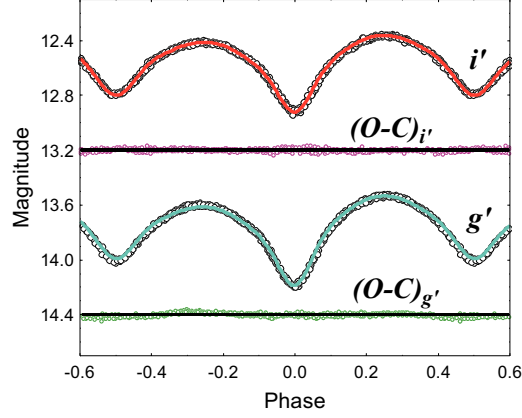


Figure 6. Same as Fig. 1 for V568 Peg.

Table 4. Parameters of the light curve solutions of the targets.

Par.	1	2	3	4	5	6
q	0.411(0.001)	2.325(0.005)	0.824(0.001)	0.624(0.006)	0.794(0.001)	0.494(0.001)
i	89.7(0.1)	89.5(0.4)	50.6(0.1)	76.0(0.2)	54.7(0.1)	76.3(0.1)
T_1	5440(48)	4520(34)	6882(35)	5361(35)	5603(41)	5734(48)
T_2	5273(15)	4410(7)	6502(14)	4972(26)	5801(15)	5409(17)
$\Omega_{1,2}$	2.553(0.004)	5.272(0.012)	3.556(0.009)	3.06(0.01)	3.373(0.004)	2.786(0.002)
fillout	0.59	0.715	0.0006	0.157	0.082	0.265
r_1	0.499	0.349	0.381	0.434	0.408	0.462
r_2	0.348	0.486	0.347	0.352	0.367	0.340
l_1	0.71	0.38	0.47	0.69	0.500	0.74
l_2/l_1	0.41	1.73	1.13	0.45	1.0	0.35

Table 5. Parameters of the cool spots on the primary components and third light contribution.

Target	β	λ	α	κ	$l_3(i')$	$l_3(g')$
1	90	270	20	0.85	0.06	0.0
2	90	90	22	0.80	0.20	0.20
3	90	270	16	0.90	0.0	0.045
4	90	240	18	0.90	0.0	0.0
5	90	90	15	0.80	0.05	0.0
6	70	75	22	0.85	0.07	0.06

in most cases (Table 5). The considerable third light contribution of V1007 Cas can be explained by the close two neighbors in the target field.

(10) The light curves of NSVS 3640326 and V1007 Cas are quite unusual: the bottoms of their MinI are flat. In order to reproduce this peculiarity, we had to adopt limb-darkening coefficients of their primary components which were considerably smaller than the values appropriate to their temperatures: $u_1(i')=0.05$, $u_1(g')=0.06$ for NSVS 3640326 and $u_1(i')=0.2$, $u_1(g')=0.3$ for V1007 Cas. In spite of numerous attempts we did not manage to reach excellent modelling of these MinI (see the residuals in Figs. 1-2) in contrast to those of the remaining targets (Figs. 3-6). This failure may be due to the huge fillout factors of these dumbbell-shaped targets (Fig. 7), as well as possible presence of an additional absorption structure as disk-like features or clouds at some Lagrangian points (a result of previous nonconservative mass transfer).

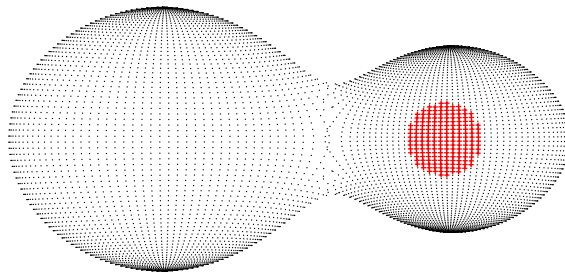


Figure 7. 3D configuration of V1007 Cas.

(11) It is well known that the determination of the mass ratio through a light-curve solution is an ambiguous approach compared to that of a radial velocity solution. However, the rapid rotation of the components of the short-period binaries is a serious obstacle to obtain a precise spectral mass ratio from measurement of their highly-broadened and blended spectral lines (Bilir *et al.*, 2005; Dall, Schmidtobreick, 2005). On the other hand, their eclipse depths depend strongly on the potentials and the mass ratios. Hence, the obtained photometric mass ratios of our targets could be considered with confidence, especially those of NSVS 3640326 and V1007 Cas corresponding to total eclipses (Mochnacki, Doughty 1972).

The sensibility of our solutions (measured by χ^2) to the mass ratio is illustrated in Fig. 8.

(12) V1007 Cas is an unusual system because its secondary component is cooler ($T_2 = 0.98 T_1$) but bigger ($r_2 = 1.39 r_1$) and more massive ($M_2 = 2.32 M_1$) than the primary. Figure 9 exhibits the complex variability of its color index ($g'-i'$) with the orbital phase.

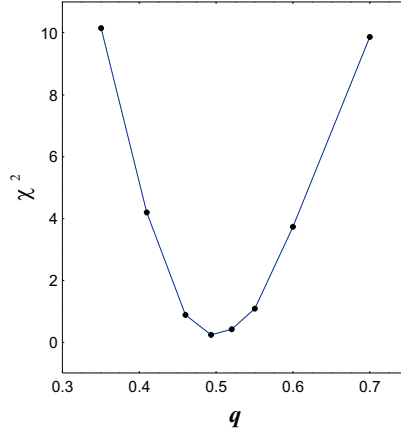


Figure 8. Sensibility of our light curve solution of V568 Peg (measured by χ^2) to the mass ratio (the remaining parameters are kept fixed at their final values).

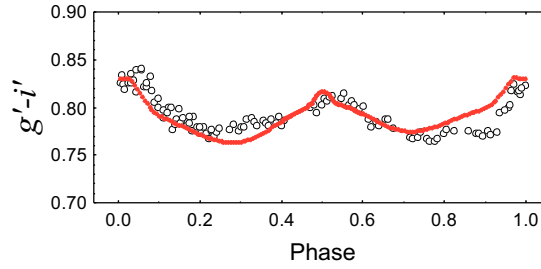


Figure 9. A $(g' - i')$ light curve of V1007 Cas and its fit.

The results of our light curve solutions can be used for an estimate of the global parameters of the targets (masses, radii and luminosities) using the statistical period-color-luminosity relation of W UMa stars and an assumption that their components are (almost) MS stars.

5. Subclassification of our targets

The contact binary stars were divided into two subtypes, A and W, according to the following criteria: (a) the ratio R/T (radius to temperature): the larger star is the hotter one for an A-type system, while the smaller star is the hotter one for a W-type system (Binnendijk, 1970; Pribulla, et al. 2003); (b) temperature T or spectral type: the A type systems are earlier than the W type binaries whose

Table 6. Subclassification of the targets.

Criterion/target	1	2	3	4	5	6
T/R	A	W	W	A	W	A
T	W	W	W	W	W	W
P	W	W	W	W	W	W
$q, l_2/l_1$	A	H/A	H/W	A	H/W	A

components are of G and K spectral type; (c) period P : the W-type binaries have shorter periods of 0.22 to 0.4 day (Smith, 1984).

According to Yildiz, Dogan (2013) the A- and the W-subtype contact binaries have different ranges of initial secondary masses: binary systems with an initial mass higher than $1.8 M_{\odot}$ become an A-subtype, while systems with initial masses lower than this become a W-subtype.

Lucy, Wilson (1979) introduced B-subtype systems whose components are in geometrical, but not thermal contact, with the temperature difference ΔT above 1000 K (Rucinski, Duerbeck, (1997).

Csizmadia, Klagyivik (2004) introduced H subtype systems (H/A and H/W) with a large mass ratio ($q \geq 0.72$) whose energy transfer is less efficient than that in other types of contact binary stars. They found that the different subtypes of W UMa's are located in different regions on the mass ratio – luminosity ratio diagram, but above the line $\lambda = q^{4.6}$ ($\lambda = l_2/l_1$) representing the mass-luminosity relation for the MS detached stars (fig. 1 in Csizmadia, Klagyivik (2004)). This is due to the overluminosity of the secondary components with respect to their current mass.

The subclassification of our targets according to the foregoing criteria is given in Table 6. Its last row shows the region of our targets on the mass ratio – luminosity ratio diagram. As expected, they are located well above the line $\lambda = q^{4.6}$. Only V1007 Cas falls well below this line, as well as below the line $\lambda = q^{0.92}$ representing the relation of Lucy (1968) for W UMa stars. Only this binary has a huge fillout factor (Fig. 7) and an "inverse" mass ratio ($q=2.32$), i.e. its secondary is cooler but more massive than the primary. These peculiarities could be taken as indications of past mass and energy transfer and a possible full merging of the components of this target in the future. All these characteristics make V1007 Cas an interesting target for follow-up spectral and photometric observations.

The subclassification of our targets (Table 6) reveals that some of them belong simultaneously to two subtypes. This result means that the proposed criteria and subdivision are ambiguous and, of course, that the stellar world is richer than one expects.

6. Conclusions

We obtained light curve solutions of six binaries with periods within 6–8 hours. One of them is a newly discovered eclipsing system.

NSVS 3640326, V1007 Cas and V0568 Peg have the biggest fillout factors and big differences of the masses of their components.

The light curves of NSVS 3640326 and V1007 Cas are quite unusual: the bottoms of their MinI are flat. In order to reproduce this peculiarity, we had to adopt limb-darkening coefficients of their primary components which were considerably smaller than the values appropriate to their temperatures. What does the negligible limb-darkening effect of these stars really mean: isothermal photospheres or some unknown mechanism? Is there a relation with the big fillout factors of these systems? Are there some additional absorbing features within their configurations?

All targets revealed the O’Connell effect that was reproduced by big cool spots on the side surfaces of their primary components. It is possible that all of them (or those of them with a big fillout factor) are at the stage of merging via ”magnetic braking” (Martin *et al.*, 2011).

V1007 Cas turned out to be well below the line representing the mass-luminosity relation for the MS stars on the mass ratio – luminosity ratio diagram. This binary has a huge fillout factor and an ”inverse” mass ratio ($q=2.32$), i.e. its secondary is cooler, but bigger and more massive, than the primary. In addition the limb-darkening effect of its primary is unusually weak. It is worth studying how these peculiarities of V1007 Cas are connected with its internal structure.

This investigation adds six new systems with estimated parameters to the family of short-period binaries. They could help to improve the statistical relations between the stellar parameters of the low-massive stars.

Acknowledgements. The research was supported partly by funds of projects RD 02-263 of Scientific Foundation of Shumen University. This publication makes use of data products from the Two Micron All Sky Survey, which is a joint project of the University of Massachusetts and the Infrared Processing and Analysis Center/California Institute of Technology, funded by the National Aeronautics and Space Administration and the National Science Foundation. This research also has made use of the SIMBAD database, operated at CDS, Strasbourg, France, NASA’s Astrophysics Data System Abstract Service, the USNOFS Image and Catalogue Archive operated by the United States Naval Observatory, Flagstaff Station (<http://www.nofs.navy.mil/data/fchpix/>) and the photometric software VPHOT operated by the AAVSO, Cambridge, Massachusetts. The authors are grateful to an anonymous referee for valuable notes and propositions.

References

Bilir, S., Karatas, Y., Demircan, O., Eker, Z.: 2005, *Mon. Not. R. Astron. Soc.* **357**, 497

- Binnendijk, L.: 1970, *Vistas Astron.* **12**, 217
- Berry, R., Burnell, J.: 2006, *The Handbook of Astronomical Image Processing with AIP4WIN2 software*, Willmann-Bell, Inc., WEB
- Coughlin, J., Lopez-Morales, M., Harrison, T., Ule, N., Hoffman, D.: 2011, *Astron. J.* **141**, 78
- Csizmadia, Sz., Klagyivik P.: 2004, *Astron. Astrophys.* **426**, 1001
- Dall, T.H., Schmidtobreick, L.: 2005, *Astron. Astrophys.* **429**, 625
- Diethelm, R.: 2013, *Inf. Bull. Variable Stars* **6042**, 1
- Drake, A.J., et al.: 2014, *Astrophys. J.* **790**, 157
- Eker, Z., Bilir, S., Yaz., E., Demircan, O., Helvacı, M.: 2008, *Astron. Nachr.* **999**, 157
- Flannery, B.P.: 1976, *Astrophys. J.* **205**, 217
- Gettel, S.J., Geske, M.T., McKay, T.A.: 2006, *Astron. J.* **131**, 621
- Khruslov, A.V.: 2008, *Perem. Zvezdy* **8**, 52
- Klagyivik, P., Csizmadia, Sz.: 2004, *PADEU* **14**, 303
- Lucy, L.B., Wilson, R.E.: 1979, *Astrophys. J.* **231**, 502
- Lucy, L.B.: 1968b, *Astron. J.* **151**, 1123
- Lucy, L.B.: 1968a, *Astrophys. J.* **151**, 877
- Lucy, L.B.: 1976, *Astrophys. J.* **205**, 208
- Martin, H.C., Spruit, H.C., Tata, R.: 2011, *Astron. Astrophys.* **535**, A50
- Mochnecki, S., Doughty, N.: 1972, *Mon. Not. R. Astron. Soc.* **156**, 51
- Otero, S.A., Wils, P., Dubovsky, P.A.: 2005, *Inf. Bull. Variable Stars* **5586**, 1
- Prsa, A., Zwitter, T.: 2005, *Astrophys. J.* **628**, 426
- Pribulla, T., Kreiner, J.M., Tremko, J.: 2003, *CAOSP* **33**, 38
- Pribulla, T., Rucinski, S.M.: 2006, *Astron. J.* **131**, 2986
- Qian, S.-B.: 2003, *Mon. Not. R. Astron. Soc.* **342**, 1260
- Robertson, J.A., Eggleton, P.P.: 1977, *Mon. Not. R. Astron. Soc.* **179**, 359
- Rucinski, S.M.: 1994, *Publ. Astron. Soc. Pac.* **106**, 462
- Rucinski, S.M.: 1996, in *The origins, evolution, and destinies of binary stars in clusters*, eds.: E.F. Milone and J.-C. Mermilliod, University of Calgary, Calgary, 270
- Rucinski, S.M., Duerbeck, H.W.: 1997, *Publ. Astron. Soc. Pac.* **109**, 1340
- Rucinski, S.M.: 1998, *Astron. J.* **116**, 2998
- Rucinski, S.M., Lu, W., Mochnecki, S.W., Ogloza, W., Stachovski, G.: 2001, *Astron. J.* **122**, 1974
- Rucinski, S.M.: 2002, *Publ. Astron. Soc. Pac.* **114**, 1124
- Samus, N.N., et al.: 2004, *VizieR Online Data Catalog: Combined General Catalogue of Variable Stars* **2250**, 0
- Smith, R.C.: 1984, *QJRAS* **25**, 405
- Stepien, K.: 2006, *Acta Astron.* **56**, 199
- Terrell, D., Gross, J., Cooney, W.R.: 2012, *Astron. J.* **143**, 99
- Tokunaga, A.T.: 2000, *Allen's astrophysical quantities*, ed. by Arthur N. Cox, p. 143, Springer, New York
- Van Hamme, W.: 1993, *Astron. J.* **106**, 2096
- Wozniak, P.R. et al.: 2004, *Astron. J.* **127**, 2436
- Yildiz, M., Dogan, T.: 2013, *Mon. Not. R. Astron. Soc.* **430**, 2029
- Zacharias, N. et al.: 2010, *Astron. J.* **139**, 2184

A. Standard stars

Table 7. List of standard stars

Label	Star ID	Other designations	RA	Dec	g'	i'
Target 1	NSVS 3640326	GSC 02793-01463	00 04 14.22	+43 18 03.4	12.506	11.801
Chk	UCAC4-667-000346	2MASS J00034969+4317099	00 03 49.71	+43 17 10.02	12.304	11.925
C1	UCAC4-667-000297	GSC 02793-01573	00 04 34.36	+43 21 55.86	11.976	11.652
C2	UCAC4-667-000274	GSC 02793-00624	00 03 27.00	+43 19 47.37	12.548	11.823
C3	UCAC4-667-000252	GSC 02793-00153	00 03 16.24	+43 23 26.59	12.019	10.845
C4	UCAC4-667-000259	GSC 02793-01607	00 03 19.74	+43 14 50.99	12.269	11.586
C5	UCAC4-666-000330	GSC 02793-01191	00 04 31.70	+43 09 10.79	12.960	12.376
C6	UCAC4-666-000340	GSC 02793/00117	00 04 41.50	+43 10 31.05	12.822	12.362
C7	UCAC4-667-000372	GSC 02793-00372	00 04 50.10	+43 17 52.47	13.450	12.851
Target 2	V1007 Cas	NSVS 3687570	00 08 03.43	+51 08 02.8	12.439	11.663
Chk	UCAC4-706-001137	GSC 03258-00336	00 07 55.75	+51 07 10.48	12.885	12.208
C1	UCAC4-706-001071	GSC 03258-00562	00 07 31.09	+51 06 18.30	12.695	11.988
C2	UCAC4-706-001208	GSC 03258-00158	00 08 20.37	+51 05 23.89	12.406	12.094
C3	UCAC4-706-001212	GSC 03258-00962	00 08 21.61	+51 07 07.81	12.603	11.964
C4	UCAC4-706-001181	GSC 03258-01296	00 08 11.31	+51 11 51.66	12.503	11.990
C5	UCAC4-706-001048	GSC 03258-00234	00 07 20.95	+51 10 51.91	12.818	10.344
C6	UCAC4-706-001053	GSC 03258-00712	00 07 22.98	+51 09 49.81	13.068	12.512
Target 3	NSVS 1776195	GSC 03684-00992	01 59 34.73	+53 02 48.2	11.424	10.738
Chk	UCAC4-716-016044	GSC 03684-01518	01 59 58.77	+53 00 28.03	13.367	11.898
C1	UCAC4-715-015419	GSC 03684-00884	01 59 52.76	+52 57 34.39	12.360	11.750
C2	UCAC4-715-015416	GSC 03684-00522	01 59 51.80	+52 58 52.96	12.672	10.568
C3	UCAC4-716-016018	GSC 03684-00414	01 59 47.87	+53 00 16.52	11.932	11.344
C4	UCAC4-715-015303	GSC 03684-01630	01 58 58.15	+52 58 00.64	11.357	10.587
C5	UCAC4-716-015945	GSC 03684-01812	01 59 11.37	+53 06 30.85	13.518	12.983
C6	UCAC4-716-016005	GSC 03684-01344	01 59 41.36	+53 05 46.92	13.630	12.812
C7	UCAC4-716-015921	GSC 03684-00838	01 58 59.18	+53 08 24.84	12.815	12.309
Target 4	UCAC4-525-135123	2MASS J20365262+1456434	20 36 52.63	+14 56 43.30	15.498	14.279
Chk	UCAC4-526-137415	-	20 36 37.27	+15 00 20.77	14.643	13.796
C1	UCAC4-525-135056	-	20 36 38.14	+14 56 26.46	14.195	12.904
C2	UCAC4-526-137452	GSC 01633-00848	20 36 46.99	+15 00 42.76	12.696	11.773
C3	UCAC4-526-137448	GSC 01633-00592	20 36 45.86	+15 01 32.84	13.453	12.809
C4	UCAC4-526-137432	-	20 36 43.26	+15 02 08.58	13.687	12.953
C5	UCAC4-525-135203	-	20 37 12.30	+14 56 31.55	15.415	14.481
C6	UCAC4-525-135208	-	20 37 13.53	+14 57 14.20	14.713	13.691
C7	UCAC4-525-135209	-	20 37 14.41	+14 57 53.33	14.255	13.375
Target 5	NSVS 113026	GSC 04599-00229	21 27 39.27	+76 39 57.6	13.122	12.122
Chk	UCAC4-833-019744	GSC 04599-00756	21 26 15.65	+76 31 27.72	13.586	12.640
C1	UCAC4-834-018508	GSC 04599-01136	21 26 53.28	+76 39 36.74	13.628	12.650
C2	UCAC4-834-018499	GSC 04599-00047	21 26 42.79	+76 41 44.43	11.626	10.910
C3	UCAC4-833-019747	GSC 04599-00345	21 26 30.61	+76 32 27.50	14.299	13.412
C4	UCAC4-833-019732	GSC 04599-00623	21 25 40.48	+76 32 33.77	12.123	11.663
C5	UCAC4-834-018484	GSC 04599-00182	21 25 58.48	+76 42 08.04	14.013	12.955
C6	UCAC4-834-018480	GSC 04599-00077	21 25 45.09	+76 38 07.46	14.756	13.934
Target 6	V0568 Peg		23 08 13.06	+33 03 03.09	13.518	12.353
Chk	UCAC4-616-135618	GSC 02755-01594	23 08 25.28	+33 03 20.67	13.538	12.866
C1	UCAC4-616-135602	GSC 02755-01799	23 08 07.80	+33 00 07.18	14.084	13.016
C2	UCAC4-616-135589	GSC 02755-00785	23 07 57.59	+33 02 49.98	12.498	11.598
C3	UCAC4-616-135579	GSC 02755-01383	23 07 47.10	+33 03 04.31	14.448	13.399
C4	UCAC4-616-135593	GSC 02755-01918	23 08 00.32	+33 06 28.34	14.680	13.484
C5	UCAC4-616-135597	GSC 02755-01040	23 08 03.04	+33 06 03.56	14.878	13.806
C6	UCAC4-616-135613	GSC 02755-00445	23 08 17.68	+33 07 59.09	14.478	13.369
C7	UCAC4-616-135636	GSC 02755-01782	23 08 31.42	+33 00 43.30	14.582	13.897